



HAL
open science

Diode-pumped sub-50-fs Kerr-lens mode-locked Yb:GdYCOB laser

Huangjun Zeng, Haifeng Lin, Zhanglang Lin, Lizhen Zhang, Zhoubin Lin, Ge Zhang, Valentin Petrov, Pavel Loiko, Xavier Mateos, Li Wang, et al.

► **To cite this version:**

Huangjun Zeng, Haifeng Lin, Zhanglang Lin, Lizhen Zhang, Zhoubin Lin, et al.. Diode-pumped sub-50-fs Kerr-lens mode-locked Yb:GdYCOB laser. *Optics Express*, 2021, 29 (9), pp.13496. 10.1364/OE.424769 . hal-03345700

HAL Id: hal-03345700

<https://hal.science/hal-03345700v1>

Submitted on 12 Oct 2021

HAL is a multi-disciplinary open access archive for the deposit and dissemination of scientific research documents, whether they are published or not. The documents may come from teaching and research institutions in France or abroad, or from public or private research centers.

L'archive ouverte pluridisciplinaire **HAL**, est destinée au dépôt et à la diffusion de documents scientifiques de niveau recherche, publiés ou non, émanant des établissements d'enseignement et de recherche français ou étrangers, des laboratoires publics ou privés.

Diode-pumped sub-50-fs Kerr-lens mode-locked Yb:GdYCOB laser

HUANGJUN ZENG,^{1,2,7} HAIFENG LIN,^{1,7} ZHANGLANG LIN,¹ LIZHEN ZHANG,¹ ZHOUBIN LIN,¹ GE ZHANG,¹ VALENTIN PETROV,³ PAVEL LOIKO,⁴ XAVIER MATEOS,^{5,6}  LI WANG,^{3,8} AND WEIDONG CHEN^{1,3,9} 

¹Key Laboratory of Optoelectronic Materials Chemistry and Physics, Fujian Institute of Research on the Structure of Matter, Chinese Academy of Sciences, Fuzhou, 350002 Fujian, China

²College of Chemistry, Fuzhou University, Fuzhou, 350116 Fujian, China

³Max Born Institute for Nonlinear Optics and Short Pulse Spectroscopy, Max-Born-Str. 2a, 12489 Berlin, Germany

⁴Centre de Recherche sur les Ions, les Matériaux et la Photonique (CIMAP), UMR 6252 CEA-CNRS-ENSICAEN, Université de Caen, 6 Boulevard du Maréchal Juin, 14050 Caen Cedex 4, France

⁵Universitat Rovira i Virgili (URV), Física i Cristal·lografia de Materials i Nanomaterials (FiCMA-FiCNA), 43007 Tarragona, Spain

⁶Serra Hünter Fellow, Spain

⁷These authors contributed equally to this work

⁸lwang@mbi-berlin.de

⁹chenweidong@fjirsm.ac.cn

Abstract: We present a sub-50-fs diode-pumped Kerr-lens mode-locked laser employing a novel “mixed” monoclinic Yb:Ca₄(Gd,Y)O(BO₃)₃ (Yb:GdYCOB) crystal as a gain medium. Nearly Fourier-limited pulses as short as 43 fs at 1036.7 nm are generated with an average power of 84 mW corresponding to a pulse repetition rate of ~70.8 MHz. A higher average power of 300 mW was achieved at the expense of the pulse duration (113 fs) corresponding to an optical-to-optical efficiency of 35.8% representing a record-high value for any Yb-doped borate crystal. Non-phase-matched self-frequency doubling is observed in the mode-locked regime with pronounced strong spectral fringes which originate from two delayed green replicas of the fundamental femtosecond pulses in the time domain.

© 2021 Optical Society of America under the terms of the [OSA Open Access Publishing Agreement](#)

1. Introduction

Yb³⁺-doped calcium rare-earth oxoborate crystals having a chemical formula Ca₄REO(BO₃)₃ (where RE = Y or Gd, abbreviated Yb:YCOB or Yb:GdCOB), are representatives of a disordered crystal family that exhibits monoclinic symmetry and belongs to the acentric *Cm* space group. They feature (i) extremely broad and smooth gain profiles supporting sub-50-fs pulses in the 1- μ m spectral range [1], which is related to their local structural disorder due to the random distribution of Gd³⁺ and/or Y³⁺ and Ca²⁺ ions over two distorted octahedral sites leading to inhomogeneous broadening of the spectral lines [2], (ii) one of the largest splitting of the ground (²F_{7/2}) manifold (>1000 cm⁻¹), which is favorable for high efficiency and low threshold laser operation without significant temperature sensitivity [3], (iii) high absorption cross-section at ~976 nm allowing for direct excitation by commercialized high-power InGaAs diode lasers into the zero-phonon-line yielding very low quantum defect (~7%), (iv) weak concentration quenching permitting high doping levels of Yb³⁺ ions in the host matrix (>20 at.%), (v) natural birefringence of the biaxial host crystals inducing anisotropic absorption and emission, which offers more flexibility in pumping and spectral bandwidth utilization, (vi) attractive thermo-optical properties [3,4] and (vii) one of the longest fluorescence lifetimes (²F_{5/2}, >2 ms) among Yb³⁺-doped

oxide crystals, which is beneficial for energy storage in Q-switched lasers and laser amplifiers [5]. All above-mentioned advantageous for high peak/average power ultrashort pulse generation with passive mode-locking technology. Semiconductor Saturable Absorber Mirror (SESAM) mode-locked (ML) thin-disk Yb:YCOB lasers produced average output powers of 4.7 and 2 W for pulse durations of 455 and 270 fs, respectively [6]. The first sub-100 fs pulse generation using Yb:GdCOB crystal was reported in 2000. Mode-locking by a SESAM generated 90 fs pulses with an average power of 40 mW at a central wavelength of 1045 nm [7]. Subsequently, 73 fs pulses with an average power of 70 mW were directly generated from a Kerr-lens mode-locked Yb:YCOB oscillator [8]. The shortest pulse duration was demonstrated in a SESAM ML Yb:YCOB laser delivering 35 fs pulses with an average power of only 44 mW [9].

Further expansion of the gain bandwidth of Yb³⁺-doped Ca₄REO(BO₃)₃ crystals can be achieved by developing novel “mixed” crystals with compositional disorder leading to additional inhomogeneous spectral broadening, smoothing and flattening of the gain profiles. This is possible, e.g., by mixing GdCOB and YCOB and/or by Lu-codoping, i.e., Yb:Gd_xY_{1-x}COB (Yb:GdYCOB), Yb:Gd_{1-x}Lu_xCOB (Yb:GdLuCOB) and Yb:Gd_xY_{1-x-y}Lu_yCOB (Yb:GdYLuCOB) [10–13]. Despite featuring both structural and compositional disorder, mixed Yb³⁺:Ca₄REO(BO₃)₃ crystals still exhibit very good potential for high-power operation both in continuous-wave (CW) and Q-switched regimes [14,15]. The first ML operation of a “mixed” Yb³⁺-doped Ca₄REO(BO₃)₃ crystal was reported in 2017. With the implementation of a SESAM as a mode locker, soliton-like pulses were generated using an Yb:GdYCOB crystal yielding a pulse duration of 161 fs at an average power of 20 mW [16].

Finally, we note that in addition to their excellent spectroscopic properties, monoclinic oxoborates are among the most efficient self-frequency-doubling (SFD) crystals due to their monoclinic *m* point group and the relatively high nonlinear coefficients *d*_{il} [17–19].

In the present work, a high-quality Yb:GdYCOB crystal was grown by the Czochralski method. The measured concentrations of the rare-earth ions amount to 9.3 at.% Yb³⁺, 23.5 at.% Gd³⁺ and 67.2 at.% Y³⁺. The compositional disorder is due to the presence of both Gd³⁺ and Y³⁺ as passive host ions and Yb³⁺ as an active dopant, corresponding to a stoichiometric chemical formula of Ca₄Gd_{0.235}Y_{0.672}Yb_{0.093}O(BO₃)₃. Yb:GdYCOB crystallizes in the monoclinic crystal system, and its optical properties are characterized in the frame of three mutually orthogonal (principal) optical indicatrix axes denoted as *X*, *Y* and *Z*. The corresponding refractive indices follow the setting *n*_{*x*} < *n*_{*y*} < *n*_{*z*}. The maximum absorption cross-section σ_{abs} for the zero-phonon-line of Yb³⁺ in the GdYCOB crystal at ~976 nm is 0.638×10^{-20} cm². We measured a FWHM of ~3.5 nm for this absorption line (for light polarization *E* || *Z*), large compared to other Yb³⁺-doped Ca₄REO(BO₃)₃ crystals (e.g., 2.2 nm for Yb:GdCOB, 2.5 nm for Yb:YCOB, 2.3 nm for Yb:GdYLuCOB [10], and 2.4 nm for Yb:GdLuCOB [11]) which facilitates pumping by high-power InGaAs diode lasers. The calculated gain cross-section spectra for light polarization *E* || *Z* and different Yb inversion levels β are shown in Fig. 1, revealing relatively flat and very broad gain profiles.

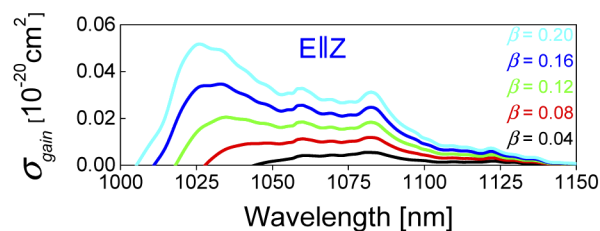


Fig. 1. Gain cross-section spectra, σ_{gain} , for Yb³⁺ ions in the “mixed” Yb:GdYCOB crystal for light polarization *E* || *Z*, β is the inversion ratio.

The promising spectroscopic features of the Yb:GdYCOB crystal motivated us to study further the mode-locking regime towards achieving shorter pulse durations. Employing a SESAM for starting and stabilizing the ML operation, in this work, we present a diode-pumped Kerr-lens mode-locked (KLM) laser using a “mixed” Yb:GdYCOB crystal. The laser exhibits also non-phase-matched SFD in the KLM femtosecond regime.

2. Experimental setup

The experimental configuration is shown in Fig. 2. CW and ML operation were investigated in a linear X-folded astigmatically compensated cavity. An uncoated 3.5-mm thick Y-cut sample with an aperture of 4 mm × 4 mm was mounted on a copper block without active cooling and placed between two dichroic folding mirrors M₁ and M₂ (radius of curvature, RoC = -100 mm) at Brewster’s angle for Z-polarization. The unpolarized pump source was a single-transverse mode, fiber-coupled diode laser which delivered up to 1.29 W of incident power at 976 nm. The measured emission bandwidth of the pump laser was 0.2 nm which is well below the bandwidth of the zero-phonon-line of the Yb:GdYCOB. The diode laser had a Fiber Bragg Grating (FBG) for wavelength locking over the entire operating range. It emitted a nearly diffraction limited beam with a beam propagation factor M² of ~1.02. The pump beam was collimated by an aspherical lens L₁ ($f = 26$ mm) and focused into the laser crystal with a waist radius of ~19 μm by using an achromatic doublet L₂ ($f = 100$ mm).

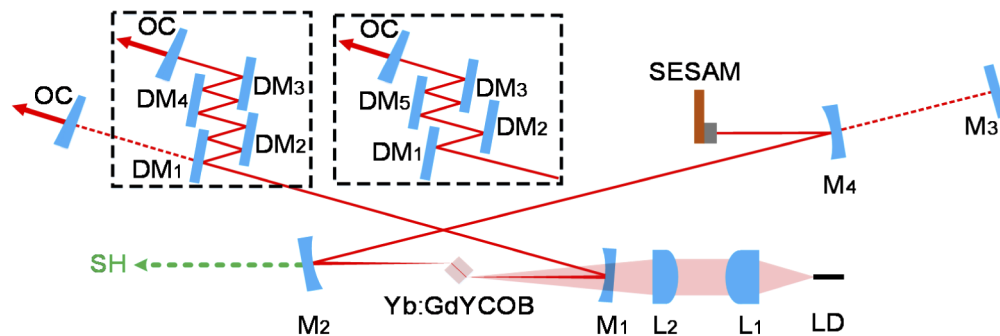


Fig. 2. Experimental arrangement of the CW and KLM Yb:GdYCOB laser. LD: fiber-coupled laser diode; L₁: collimating aspherical lens; L₂: focusing achromatic doublet; M₁-M₂: concave dichroic mirrors; M₃: flat rear mirror in CW operation; DM₁-DM₅: dispersive mirrors; OC: output coupler; SH: second-harmonic output.

3. Continuous-wave operation

The CW laser performance of the Yb:GdYCOB crystal was evaluated with a four-mirror cavity including a flat rear mirror M₃ and a plane-wedged output coupler (OC). Using the ABCD formalism, we estimated the radii of the laser mode inside the crystal as 21.4 and 37 μm in the sagittal and tangential planes, respectively. Five OCs having transmissions at the laser wavelength T_{oc} in the range 0.4% . . . 10% were used, as shown in Fig. 3(a). The measured single-pass pump absorption under lasing conditions only slightly varied with the OC being between 65% and 71%. The lowest laser threshold for CW operation amounted to 25.3 mW of absorbed pump power (for the smallest $T_{oc} = 0.4%$). The maximum output power of 328.5 mW was achieved for the 4.5% OC at an absorbed power of 628.5 mW, corresponding to a slope efficiency of 56.6%. The laser wavelength in CW regime experienced a blue-shift with increasing the transmission of the OC from 1052.5 to 1031.1 nm, as shown in Fig. 3(b). The total resonator round trip losses δ (reabsorption losses excluded) as well as the intrinsic slope efficiency η_0 (accounting for mode

matching efficiency and quantum efficiency) were estimated with the Caird analysis by fitting the measured slope efficiency as a function of the OC reflectivity $1 - T_{OC}$ [20]. The fitting results and best fit curve are shown in Fig. 3(c), giving the values of $\eta_0 = 71.1\%$ and $\delta = 0.83\%$. This result suggests a well-optimized resonator design and good quality of the laser crystal. A SF10 Brewster prism was inserted close to the OC for wavelength tuning in the CW regime. With the 0.4% OC, a broad tuning range of ~ 92 nm was achieved as shown in Fig. 3(d).

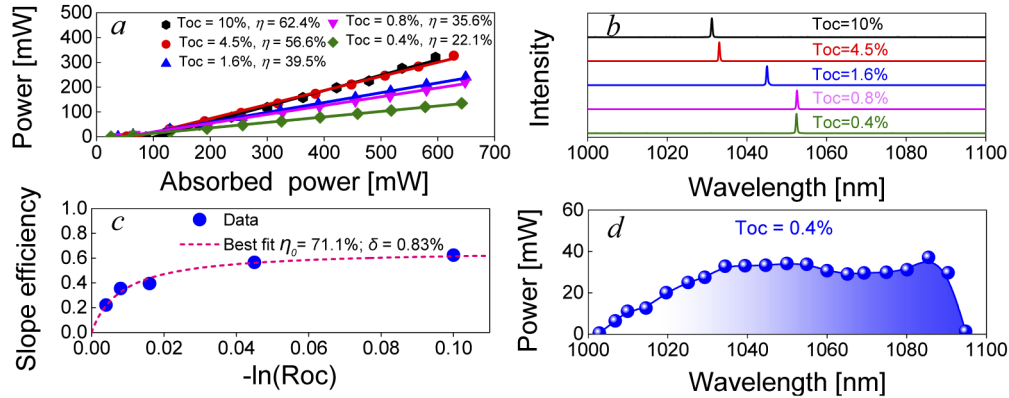


Fig. 3. CW laser performance of the Yb:GdYCOB crystal for different OCs (a); measured laser spectra in the CW regime (b), slope efficiency as a function of the OC reflectivity $1 - T_{OC}$ (c), and spectral tuning obtained with a SF10 prism in the CW regime for $T_{OC} = 0.4\%$ (d).

4. Mode-locked operation

For ML operation, M_3 was replaced by a concave mirror M_4 ($RoC = -100$ mm) to create a second beam waist in one of the cavity arms where the SESAM was implemented. A SESAM (Batop GmbH) having a modulation depth of 1.2% and a relaxation time of ~ 1 ps, was used for starting and stabilizing the ML operation. The intracavity group delay dispersion (GDD) was managed by a set of flat dispersive mirrors (DMs) having different negative GDD (-250 fs², -100 fs² and -55 fs² per bounce) for compensation of the material GDD and balancing the self-phase modulation (SPM) to form steady-state soliton-like pulses, cf. Figure 2 [21]. The total roundtrip material GDD due to the 3.5-mm thick crystal amounted to ~ 585 fs² at 1036 nm (for $E \parallel Z$), estimated by averaging the refractive indices of YCOB and GdCOB [22,23].

ML operation was initially investigated by applying eight bounces (single pass) on the flat DMs ($DM_1 - DM_4$, $DM_1 = DM_2 = -250$ fs², $DM_3 = DM_4 = -100$ fs²) giving a total round-trip GDD of -2800 fs². Stable and self-starting soliton ML operation was initiated and stabilized by the SESAM with a 4.5% OC. The maximum average output power amounted to 252 mW for an absorbed power of 882 mW. The optical spectrum was centered at 1036.4 nm with a sech²-fitted spectral FWHM of 7.4 nm, as shown in Fig. 4(a). Figure 4(b) shows the corresponding intensity autocorrelation trace which was well fitted by assuming a sech² pulse profile giving a duration of 161 fs (FWHM). Excellent sech² shaped spectral and temporal profiles indicating soliton-like ML pulses were achieved, as well as near Fourier-limited pulses with a time-bandwidth product of 0.333. Subsequently, soft-aperture Kerr-lens effect was introduced by gradually enlarging the laser mode size inside the Yb:GdYCOB crystal through changing the separation between the pump mirror M_1 and M_2 while keeping the same level of absorbed power (882 mW) [24]. A significant spectral broadening was observed when translating the folding mirror M_2 away from the pump mirror M_1 . The FWHM of the ML spectrum increased from 7.4 to 17.7 nm with the

central wavelength experiencing a red-shift of 3.3 nm, i.e., from 1036.4 to 1039.7 nm, as shown in Fig. 4(c). Assuming a sech^2 temporal profile, the measured intensity autocorrelation trace gave a pulse duration of 70 fs, see Fig. 4(d). The average power dropped to 192 mW at a pulse repetition rate of ~ 75 MHz. The spectral broadening and pulse shortening in the ML regime indicates that the KLM became the dominant pulse shaping mechanism, and the SESAM simply played the role of a starter and stabilizer. The corresponding on-axis peak intracavity intensity in the Yb:GdYCOB crystal amounted to ~ 123 GW/cm².

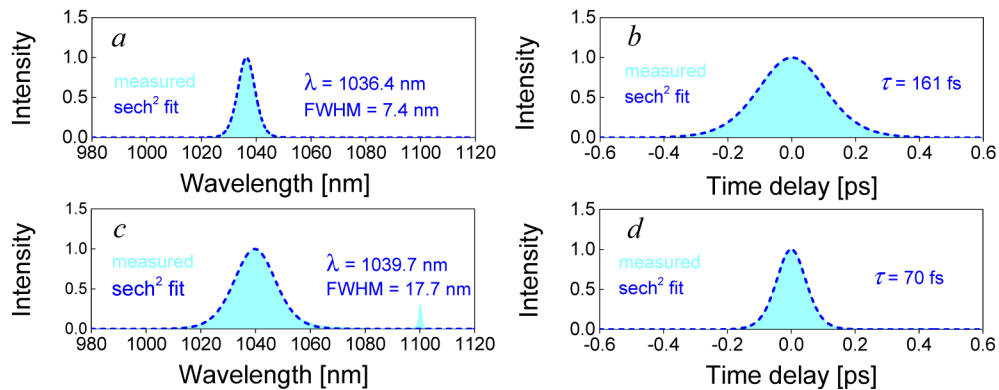


Fig. 4. Characterization of the transition of the ML Yb:GdYCOB laser from SESAM ML to KLM with $T_{oc} = 4.5\%$. ML optical spectra with sech^2 fit indicating soliton pulses: (a) SESAM ML and (c) KLM; autocorrelation traces with sech^2 fit: (b) SESAM ML and (d) KLM.

Soft-aperture KLM was further confirmed by monitoring the changes in the output beam profile, as shown in Fig. 5. An IR Camera (DataRay, WinCamD) was placed at ~ 1.8 m from the OC for recording the far-field beam profiles. When mode-locking was initiated by the SESAM without assistance from Kerr lensing, cf. Figures 4(a) and 4(b), the beam profile in the far-field had a diameter of $4.2 \text{ mm} \times 4 \text{ mm}$, as shown in Fig. 5(a). The transition to dominating soft-aperture KLM, i.e., strong self-focusing inside the Yb:GdYCOB crystal with soft-aperture Kerr-lens effect, cf. Figures 4(c) and (d), is confirmed by the shrinking of the beam diameter in the far-field to $4.2 \text{ mm} \times 2.9 \text{ mm}$, Fig. 5(b).

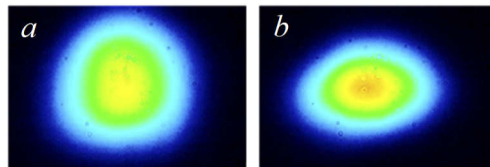


Fig. 5. ML Yb:GdYCOB laser transition from SESAM ML to KLM by changing the mirror separation $M_1 - M_2$ ($T_{oc} = 4.5\%$). Far-field beam profiles: (a) SESAM ML and (b) KLM.

Even shorter pulse durations could be realized by reducing the OC transmission to 2.5% at the expense of the average power. KLM pulses had a sech^2 fitted spectral FWHM of 18.5 nm at 1039 nm. The deconvolved FWHM of the pulse duration was 66 fs from the measured intensity autocorrelation trace, at an average output power of 127 mW for an absorbed power of 912 mW. The corresponding time-bandwidth product amounted to 0.339. In this case, the on-axis intracavity intensity on the Yb:GdYCOB crystal reached ~ 157 GW/cm². Power scaling of the KLM laser was achieved by using the 10% OC with a maximum average output power of 300 mW for an absorbed power of 837 mW. The corresponding optical-to-optical efficiency

reached to 35.8% with respect to the absorbed power. To the best of our knowledge, this represents the highest ML conversion efficiency from any Yb-doped borate crystal. The ML pulses had a duration of 113 fs (FWHM) by assuming a sech^2 temporal profile. The sech^2 -fitted FWHM of the KLM spectrum was 10.4 nm and the central wavelength was 1034.1 nm. The resulting time-bandwidth product was 0.329 and the calculated on-axis intracavity intensity in the Yb:GdYCOB crystal amounted to 24.7 GW/cm².

The shortest pulses could be achieved by applying six bounces (single pass) on the flat DMs ($\text{DM}_1 = \text{DM}_2 = -250 \text{ fs}^2$, $\text{DM}_3 = -100 \text{ fs}^2$, $\text{DM}_5 = -55 \text{ fs}^2$) giving a total round-trip GDD of -1620 fs^2 and using a 2.5% OC. Pulses as short as 50 fs were directly generated from the KLM Yb:GdYCOB laser with a sech^2 fitted spectral FWHM of 26.5 nm and spectrum centered at 1036.7 nm, as shown in Fig. 6(a). The corresponding time bandwidth product was 0.37. The slightly chirped pulses were subjected to externally linearly chirped compensated with two DMs of -200 fs^2 in a single pass. This resulted in a deconvolved duration with a sech^2 -fitted temporal profile of 43 fs (FWHM) from the intensity autocorrelation trace, as shown in Fig. 6(b). The long-span autocorrelation scan (40-ps) which is shown at the inset in Fig. 6(b) is an evidence for single-pulse operation without any pedestals or multi-pulses. An average output power of 84 mW was obtained for an absorbed pump power of 912 mW. The corresponding time-bandwidth product amounted to 0.318, very close to the value for transform-limit pulses of sech^2 -shape (0.315). In this case, the on-axis intracavity peak intensity in the Yb:GdYCOB crystal amounted to 228 GW/cm². The CW-ML pulse train was characterized by a radio-frequency (RF) spectrum analyzer. The recorded RF spectra for the fundamental beat note at $\sim 70.8 \text{ MHz}$ with a resolution bandwidth (RBW) of 250 Hz and a 1-GHz-wide span (RBW: 100 kHz) proving the stability of the KLM Yb:GdYCOB laser are shown in Figs. 6(c) and 6(d). The very high signal-to-noise ratio above 77 dBc of the fundamental beat-note and the absence of any spurious modulation confirm the stable CW-ML operation of the Yb:GdYCOB laser for the shortest pulse durations.

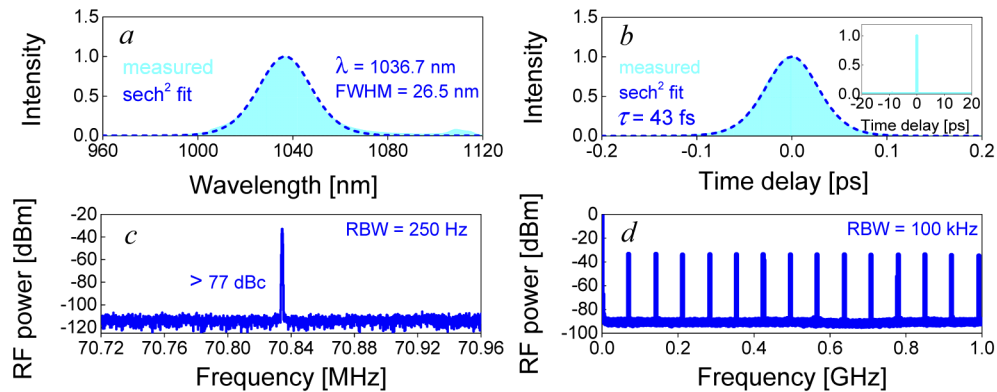


Fig. 6. Measured ML spectrum of the Yb:GdYCOB laser with $T_{\text{OC}} = 2.5\%$ (a) and intensity autocorrelation trace with a sech^2 -fit (b). Inset: autocorrelation trace in the time span of 40 ps; RF spectra of the ML Yb:GdYCOB laser: fundamental beat note (c) and 1-GHz span (d).

Due to the non-centrosymmetric structure of the Yb:GdYCOB crystal, non-phase matched self-frequency doubling of femtosecond pulses was observed during the KLM operation. Applying a 0.8% OC, a second-harmonic (SH) spectrum with strong interference fringes was recorded for a pulse duration of the fundamental radiation of 47 fs at 1036.6 nm obtained directly from the laser and a sech^2 fitted spectral FWHM of 25.6 nm, as shown in Fig. 7. The ML laser generated an average power of 32 mW for an absorbed power 921 mW. The well-defined spectral fringes in the SH spectrum with 1.07 nm fringe spacing originate from the interference of two green pulses in the Yb:GdYCOB crystal under the non-phase matching conditions and strong group velocity

mismatch (GVM) with the fundamental [25]. This value is in fair agreement with the calculated one of 0.77 nm from the GVM between the fundamental and SH using the Sellmeier equations for undoped YCOB. The measured average green power behind M_2 amounted to 265 μ W. Having in mind the transmission of this mirror the calculated conversion efficiency is about 10^{-4} which is rather high for a non-phase matched process. Similar SH powers were reported in [7] but the Yb:GdCOB sample employed was cut for phase-matching and although the wavelength was not optimum for this the strong narrowing of the SH spectrum indicates that the process was partially phase-matched and the SH pulses were broadened due to spectral acceptance limitations. In our case the SH had the same polarization as the fundamental and the spectral narrowing factor corresponds exactly to the expected 4-fold reduction in nanometers and the increase due to the pulse shortening effect in low-signal SH generation (e.g. $\sqrt{2}$ times for Gaussian pulse shape giving). This indicates a purely non-phase-matched nonlinear process leading preserved or shorter pulse durations at the SH. No spectral narrowing of the SH was observed on the other hand also in [26] with a ML Yb:YCOB laser. While the polarization specifications in this work seem erroneous which precludes the explanation of the unrealistically high SH power obtained, in our case the high conversion efficiency can be attributed to the utilization of the highest nonlinear coefficient d_{33} of this family of crystals [27]. The coherence length for SH generation based on d_{33} and d_{13} is similar and amounts to $\sim 8 \mu\text{m}$. The linear polarization along the Z axis observed for the SH can be attributed then to the higher coefficient d_{33} (exceeding d_{13} two times or more according to the literature) whose value is above 1 pm/V and the reflection losses for the s-polarization at the exit crystal face which is at Brewster's angle only for p-polarization.

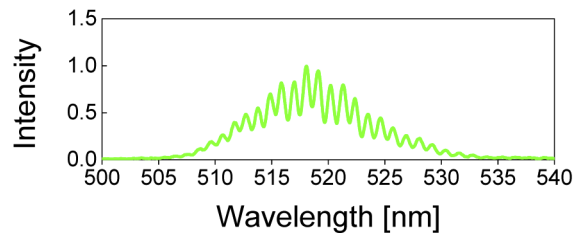


Fig. 7. Measured non-phase matched self-frequency doubling spectrum after the folding mirror (M_1) during the KLM operation of the Yb:GdYCOB laser.

5. Conclusion

In conclusion, we demonstrated the first soft-aperture KLM operation of the “mixed” calcium rare-earth oxoborate crystal, Yb:GdYCOB. Almost Fourier-transform limited pulses as short as 43 fs at 1036.7 nm were generated with an average power of 84 mW for a pulse repetition rate of 70.8 MHz. Power scaling was realized using 10% OC. A maximum average power of 300 mW was achieved for a conversion efficiency of 35.8% in the KLM regime with respect to the absorbed pump power. The non-phase-matched self-frequency doubling of femtosecond pulses was also observed in the KLM regime with pronounced spectral fringes.

Funding. National Natural Science Foundation of China (61975208, 61905247, 61575199, 51761135115, 61850410533); Deutsche Forschungsgemeinschaft (PE 607/14-1); Sino-German Scientist Cooperation and Exchanges Mobility Program (M-0040).

Disclosures. The authors declare no conflicts of interest.

Data availability. Data underlying the results presented in this paper are not publicly available at this time but may be obtained from the authors upon reasonable request.

References

1. F. Druon, F. Balembois, and P. Georges, "New laser crystals for the generation of ultrashort pulses," *C. R. Phys.* **8**(2), 153–164 (2007).
2. F. Mougel, K. Dardenne, G. Aka, A. Kahn-Harari, and D. Vivien, "Ytterbium-doped $\text{Ca}_4\text{GdO}(\text{BO}_3)_3$: An efficient infrared laser and self-frequency doubling crystal," *J. Opt. Soc. Am. B* **16**(1), 164–172 (1999).
3. F. Druon, F. Balembois, P. Georges, A. Brun, A. Courjaud, C. Honninger, F. Salin, A. Aron, F. Mougel, G. Aka, and D. Vivien, "Generation of 90-fs pulses from a mode-locked diode-pumped $\text{Yb}^{3+}:\text{Ca}_4\text{GdO}(\text{BO}_3)_3$ laser," *Opt. Lett.* **25**(6), 423–425 (2000).
4. P. Loiko, X. Mateos, Y. Wang, Z. Pan, K. Yumashev, H. Zhang, U. Griebner, and V. Petrov, "Thermo-optic dispersion formulas for YCOB and GdCOB laser host crystals," *Opt. Mater. Express* **5**(5), 1089–1097 (2015).
5. P. Loiko, J. M. Serres, X. Mateos, H. H. Yu, H. J. Zhang, J. H. Liu, K. Yumashev, U. Griebner, V. Petrov, M. Aguilo, and F. Diaz, "Thermal lensing and multiwatt microchip laser operation of Yb:YCOB crystals," *IEEE Photon. J.* **8**(3), 1–12 (2016).
6. C. Kränkel, R. Peters, K. Petermann, P. Loiseau, G. Aka, and G. Huber, "Efficient continuous-wave thin disk laser operation of Yb: $\text{Ca}_4\text{YO}(\text{BO}_3)_3$ in E parallel to Z and E parallel to X orientations with 26 W output power," *J. Opt. Soc. Am. B* **26**(7), 1310–1314 (2009).
7. O. H. Heckl, C. Kränkel, C. R. E. Baer, C. J. Saraceno, T. Sudmeyer, K. Petermann, G. Huber, and U. Keller, "Continuous-wave and modelocked Yb:YCOB thin disk laser: first demonstration and future prospects," *Opt. Express* **18**(18), 19201–19208 (2010).
8. Z. Gao, J. Zhu, W. Tian, J. Wang, Z. Zhang, Z. Wei, H. Yu, H. Zhang, and J. Wang, "Generation of 73 fs pulses from a diode pumped Kerr-lens mode-locked Yb: $\text{YCa}_4\text{O}(\text{BO}_3)_3$ laser," *Opt. Lett.* **39**(20), 5870–5872 (2014).
9. A. Yoshida, A. Schmidt, V. Petrov, C. Fiebig, G. Erbert, J. H. Liu, H. J. Zhang, J. Y. Wang, and U. Griebner, "Diode-pumped mode-locked Yb:YCOB laser generating 35 fs pulses," *Opt. Lett.* **36**(22), 4425–4427 (2011).
10. F. Liu, L. Dong, J. Chen, and J. Liu, "Spectroscopic and lasing properties of a mixed (Yb, Y, Lu, Gd) calcium oxyborate crystal: $\text{Yb}_{0.19}\text{Y}_{0.34}\text{Lu}_{0.12}\text{Gd}_{0.35}\text{Ca}_4\text{O}(\text{BO}_3)_3$," *J. Lumin.* **232**, 117789 (2021).
11. F. Liu, L. Dong, J. Chen, S. Cao, H. Xu, and J. Liu, "Growth, spectroscopic properties and efficient laser action of an $\text{Yb}_{0.09}\text{Lu}_{0.13}\text{Gd}_{0.78}\text{Ca}_4\text{O}(\text{BO}_3)_3$ crystal," *CrystEngComm* **22**(36), 6026–6033 (2020).
12. Y. Zhang, Z. Lin, Z. Hu, and G. Wang, "Growth and spectroscopic properties of $\text{Yb}^{3+}:\text{Gd}_{0.5}\text{Y}_{0.5}\text{Ca}_4\text{O}(\text{BO}_3)_3$ crystal," *J. Alloys Compd.* **390**(1–2), 194–196 (2005).
13. Y. Zhang, B. Wei, and G. Wang, "Spectroscopic properties of Yb^{3+} -doped $\text{Ca}_4\text{Gd}_{0.5}\text{Y}_{0.5}\text{O}(\text{BO}_3)_3$ single crystals," *Phys. Status Solidi A* **207**(6), 1468–1473 (2010).
14. L. Dong, F. Liu, J. Chen, and J. Liu, "Highly efficient continuous-wave and passively Q-switched Yb:YLuGdCOB compact lasers," *Opt. Express* **29**(2), 1838–1850 (2021).
15. X. Chen, H. Xu, W. Han, L. Wang, J. Liu, H. Yu, and H. Zhang, "Spectroscopic properties and high-power laser operation of $\text{Yb}_{0.14}\text{Y}_{0.77}\text{Gd}_{0.09}\text{Ca}_4\text{O}(\text{BO}_3)_3$ mixed crystal," *Opt. Mater.* **55**, 33–37 (2016).
16. H. F. Lin, G. Zhang, L. Z. Zhang, Z. B. Lin, F. Pirzio, A. Agnesi, V. Petrov, and W. D. Chen, "SESAM mode-locked Yb:GdYCOB femtosecond laser," *Opt. Mater. Express* **7**(10), 3791–3795 (2017).
17. F. Khaled, P. Loiseau, G. Aka, and L. Gheorghie, "Rise in power of Yb:YCOB for green light generation by self-frequency doubling," *Opt. Lett.* **41**(15), 3607–3610 (2016).
18. Q. Fang, D. Lu, H. Yu, H. Zhang, and J. Wang, "Self-frequency-doubled vibronic yellow Yb:YCOB laser at the wavelength of 570 nm," *Opt. Lett.* **41**(5), 1002–1005 (2016).
19. D. Lu, Q. Fang, X. Yu, X. Han, J. Wang, H. Yu, and H. Zhang, "Power scaling of the self-frequency-doubled quasi-two-level Yb:YCOB laser with a 30% slope efficiency," *Opt. Lett.* **44**(21), 5157–5160 (2019).
20. J. A. Caird, S. A. Payne, P. Staber, A. Ramponi, L. Chase, and W. F. Krupke, "Quantum electronic-properties of the $\text{Na}_3\text{Ga}_2\text{Li}_3\text{F}_{12}:\text{Cr}^{3+}$ laser," *IEEE J. Quantum Electron.* **24**(6), 1077–1099 (1988).
21. F. Kartner, I. Jung, and U. Keller, "Soliton mode-locking with saturable absorbers," *IEEE J. Select. Topics Quantum Electron.* **2**(3), 540–556 (1996).
22. P. Segonds, B. Boulanger, B. Menaert, J. Zaccaro, J. P. Salvestrini, M. D. Fontana, R. Moncorge, F. Poree, G. Gadret, J. Mangin, A. Brenier, G. Boulon, G. Aka, and D. Pelenc, "Optical characterizations of $\text{YCa}_4\text{O}(\text{BO}_3)_3$ and $\text{Nd}:\text{YCa}_4\text{O}(\text{BO}_3)_3$ crystals," *Opt. Mater.* **29**(8), 975–982 (2007).
23. G. Aka, A. Kahn-Harari, F. Mougel, D. Vivien, F. Salin, P. Coquelin, P. Colin, D. Pelenc, and J. P. Damelet, "Linear- and nonlinear-optical properties of a new gadolinium calcium oxoborate crystal, $\text{Ca}_4\text{GdO}(\text{BO}_3)_3$," *J. Opt. Soc. Am. B* **14**(9), 2238–2247 (1997).
24. T. Brabec, C. Spielmann, P. Curley, and F. Krausz, "Kerr lens mode locking," *Opt. Lett.* **17**(18), 1292–1294 (1992).
25. P. Trabs, F. Noack, A. S. Aleksandrovsky, A. I. Zaitsev, N. V. Radionov, and V. Petrov, "Spectral fringes in non-phase-matched SHG and refinement of dispersion relations in the VUV," *Opt. Express* **23**(8), 10091–10096 (2015).
26. Z.-Y. Gao, J.-F. Zhu, Z.-M. Wu, Z.-Y. Wei, H.-H. Yu, H.-J. Zhang, and J.-Y. Wang, "Tunable second harmonic generation from a Kerr-lens mode-locked Yb: $\text{YCa}_4\text{O}(\text{BO}_3)_3$ femtosecond laser," *Chin. Phys. B* **26**(4), 044202 (2017).
27. P. Tzankov and V. Petrov, "Effective second-order nonlinearity in acentric optical crystals with low symmetry," *Appl. Opt.* **44**(32), 6971–6985 (2005).